

See discussions, stats, and author profiles for this publication at: <https://www.researchgate.net/publication/51853045>

# Dual-Modality Single Particle Orientation and Rotational Tracking of Intracellular Transport of Nanocargos

ARTICLE in ANALYTICAL CHEMISTRY · DECEMBER 2011

Impact Factor: 5.64 · DOI: 10.1021/ac202824v · Source: PubMed

CITATIONS

8

READS

41

## 4 AUTHORS:



**Wei Sun**

Washington University

41 PUBLICATIONS 644 CITATIONS

SEE PROFILE



**Yan Gu**

Harvard University

12 PUBLICATIONS 162 CITATIONS

SEE PROFILE



**Gufeng Wang**

North Carolina State University

53 PUBLICATIONS 1,206 CITATIONS

SEE PROFILE



**Ning jian Fang**

Ivy university

68 PUBLICATIONS 965 CITATIONS

SEE PROFILE

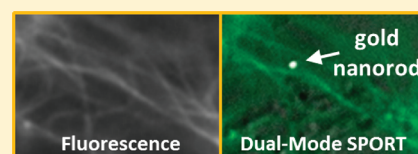
# Dual-Modality Single Particle Orientation and Rotational Tracking of Intracellular Transport of Nanocargos

Wei Sun,<sup>†</sup> Yan Gu, Gufeng Wang,<sup>‡</sup> and Ning Fang\*

Ames Laboratory, U.S. Department of Energy, and Department of Chemistry, Iowa State University, Ames, Iowa 50011, United States

**S** Supporting Information

**ABSTRACT:** The single particle orientation and rotational tracking (SPORT) technique was introduced recently to follow the rotational motion of plasmonic gold nanorod under a differential interference contrast (DIC) microscope. In biological studies, however, cellular activities usually involve a multiplicity of molecules; thus, tracking the motion of a single molecule/object is insufficient. Fluorescence-based techniques have long been used to follow the spatial and temporal distributions of biomolecules of interest thanks to the availability of multiplexing fluorescent probes. To know the type and number of molecules and the timing of their involvement in a biological process under investigation by SPORT, we constructed a dual-modality DIC/fluorescence microscope to simultaneously image fluorescently tagged biomolecules and plasmonic nanoprobe in living cells. With the dual-modality SPORT technique, the microtubule-based intracellular transport can be unambiguously identified while the dynamic orientation of nanometer-sized cargos can be monitored at video rate. Furthermore, the active transport on the microtubule can be easily separated from the diffusion before the nanocargo docks on the microtubule or after it undocks from the microtubule. The potential of dual-modality SPORT is demonstrated for shedding new light on unresolved questions in intracellular transport.



Microtubules are one component of the cytoskeleton network within the cytoplasm of mammalian cells.<sup>1</sup> They not only maintain a cell's shape but also sustain specific cellular functions through serving as the moving tracks in intracellular transport.<sup>2,3</sup> For example, in neurons, specialized proteins manufactured for signaling are transported from the cell body toward the axon tip, while endocytic vesicles at the axon tip move toward the cell body through retrograde transport.<sup>4</sup> These transport processes are accomplished by kinesin and dynein motor proteins through converting chemical energy from hydrolysis of adenosine triphosphate (ATP) into mechanical work. Kinesin and dynein motor proteins transport cargos in the opposite directions by "walking" on the intracellular microtubule network.<sup>4</sup> The *in vitro* transport behavior of motor proteins has been studied extensively, and the predominant 8 nm steps of kinesin and dynein on the microtubules were identified.<sup>5–14</sup> However, the understanding of the more complicated *in vivo* transport, which involves multiple intracellular regulation pathways and multimotor coordination in a single transport event, is still limited.<sup>11,15,16</sup>

We recently introduced the single particle orientation and rotational tracking (SPORT)<sup>17,18</sup> technique, which utilizes the gold nanorod probes<sup>19–22</sup> and transmitted-light differential interference contrast (DIC) microscopy,<sup>23,24</sup> to follow the rotational motion of nano-objects in living cells. A DIC microscope has two polarizers and two Nomarski prisms inserted in the light path of a bright field microscope. The first Nomarski prism produces two independent orthogonal vibration beams. They generate two intermediate images of a sample. Then, the second Nomarski prism laterally shifts the two intermediate images and projects their orthogonal vibration light components to the vibration direction of the second polarizer where

the final image with enhanced amplitude contrast is formed. In DIC microscopy, the optically anisotropic gold nanorod shows unique image patterns depending on its 3D orientation.

Using SPORT, we have shown that nanocargos tend to maintain their orientation relative to the microtubule tracks during the active transport in living mammalian cells,<sup>17</sup> where cytoplasmic microtubules are usually composed of 13 linear protofilaments.<sup>25</sup> An immediate question following that study was how to identify the microtubule-based transport from other types of movements, such as Brownian motion and the actin filament-based transport. Moreover, until now, little is known for the dynamics of cargo orientation at the transition stages, e.g., at the moments of cargo docking onto and undocking from the microtubule tracks, and at temporary pauses during the transport. This information is crucial to understand the motor–regulator and motor–motor interactions, which are currently under intense investigation.<sup>11,15</sup> In the present study, the dual-modality (DIC and fluorescence) SPORT technique was introduced to provide new opportunities to acquire insights to these questions.

## ■ EXPERIMENTAL SECTION

**Dual-Modality DIC/Fluorescence Microscope.** An upright Nikon Eclipse 80i microscope equipped with a heating stage was used in this study. This microscope was modified to operate in DIC mode, epi-fluorescence mode, or DIC/fluorescence dual-mode. When the microscope was operated in DIC mode, a

**Received:** October 25, 2011

**Accepted:** December 5, 2011

**Published:** December 5, 2011



set of 2 Nomarski prisms, 2 polarizers, and a quarter-wave plate were installed. The samples were illuminated through an oil immersion condenser (numerical aperture 1.40), and the optical signals were collected with a 100× Plan Apo/1.40 oil immersion objective. The DIC images at a selected wavelength were collected by inserting the corresponding bandpass filter into the light path of the microscope. The optical filters were obtained from Thorlabs (Newton, NJ) or Semrock (Rochester, NY). When the Nikon microscope was operated in epi-fluorescence mode, the samples were excited with a mercury lamp with proper band-pass filters applied in the excitation and emission channels. When the microscope was operated in DIC/fluorescence dual-mode, the instrument was set up as in Figure 1. A dual-view

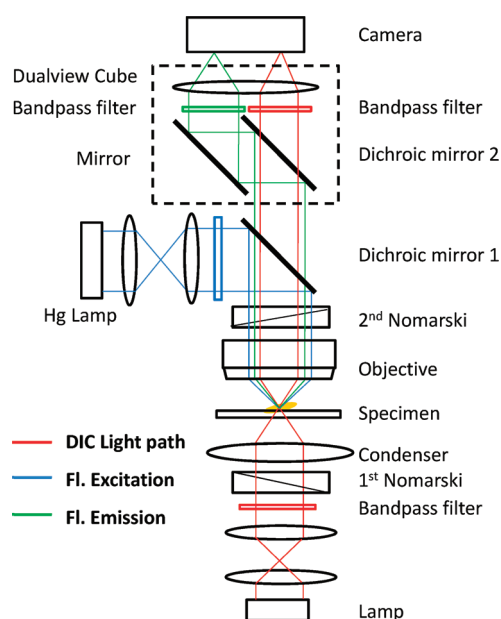


**Figure 1.** Optical path of the dual-modality DIC/fluorescence microscope. The red lines represent the optical path of a conventional Nomarski-type DIC microscope. The blue and green lines represent the fluorescence excitation and emission optical paths of an epi-fluorescence microscope, respectively.

filter cube (Photometrics, Tucson, AZ) was installed at the microscope's exit port to split the output signals at two selected wavelengths: one for the DIC image and the other for the fluorescence image. The two images were then projected onto different portions of the same camera chip and collected simultaneously. An Andor iXon<sup>EM</sup> + 897 EMCCD camera (512 × 512 imaging array and 16 × 16 μm pixel size) was used to record the dynamic intracellular transport at 32 frames per second. A rotary motor from Sigma Koki (model no. SGSP-60YAM) was coupled to the microscope stage to control the z-position of the sample. The EMCCD camera and the stage were synchronized by a homemade computer program. MATLAB and NIH ImageJ were used to analyze the collected images and videos.

**Preparation of Surface-Modified Gold Nanorods for Cell Experiments.** Cell-penetrating peptide TAT-coated gold nanorods were modified from cetyl trimethylammonium bromide (CTAB)-capped (25 nm × 73 nm,  $1.3 \times 10^{11}$  particles/mL, Nanopartz) gold nanorods. The size distribution and geometric profile were evaluated with transmission electron microscope and agreed well with the manufacturer's data. To functionalize the surface of CTAB-coated gold nanorods with TAT 47-57

peptide (sequence: YGRKKRRQRRR; AnaSpec, San Jose, CA), a NHS-PEG disulfide linker (Sigma-Aldrich) was used by following a published procedure.<sup>26</sup> The NHS-PEG disulfide linker has both disulfide and succinimidyl functionalities for respective chemisorption onto gold and facile covalent coupling of TAT peptide. Briefly, excessive surfactant was first removed from 1.0 mL of the gold nanorod solution by centrifugation at 3000g for 10 min, and the particles were resuspended in 1.0 mL of 2 mM borate buffer. A proper amount of fresh NHS-PEG disulfide solution (in dimethyl sulfoxide) was added to reach a final thiol concentration of 0.2 mM and reacted with the gold nanorods for 2 h. The solution was then cleaned by centrifugation and resuspended in 1.0 mL of 2 mM borate buffer. For TAT-modified gold nanorods, 2.0 μg of TAT peptide was added to the gold colloidal solution and reacted for 8 h. The gold nanorods were then blocked by adding 100 μL of 10% BSA solution (2 mM borate buffer) for over 8 h. Before use, the colloidal gold nanorod probes were cleaned by centrifugation and resuspended in 500 μL of 1% BSA (2 mM borate buffer). The concentrated gold colloidal solution was diluted in cell culture medium to a final concentration of  $4.3 \times 10^9$  particles/mL for incubation with cells.

**Cell Culture and Intracellular Transport of Gold Nanorods.** A549 human lung cancer cell line was purchased from American Type Culture Collection (CCL-185, Manassas, VA). The cells were plated in a T25 cell culture flask (Corning) and grown in cell culture medium supplemented with 10% fetal bovine serum (FBS) in a cell culture incubator (37 °C, 5% CO<sub>2</sub>). When subculturing, 150 μL of cell suspension solution was transferred to a 22 mm × 22 mm poly-L-lysine (PLL)-coated coverslip, housed in a 35-mm Petri dish (Corning). The Petri dish was left in the incubator for 1 h to let the cells attach to the coverslip. After 1.5 mL of the cell culture medium with 10% FBS supplement was added to immerse the coverslip, the Petri dish was incubated again for 24 h. The surface-modified gold nanorods were diluted in cell culture medium to a proper concentration and incubated with cells for 1–8 h as desired. After incubation, the microtubules were stained with Tubulin Tracker Green Reagent (T34075, Invitrogen, Carlsbad, CA) for 30 min in the incubator according to the protocol provided by Invitrogen. The coverslip with cells was then observed under the modified dual-modality DIC/fluorescence microscope.

## RESULTS AND DISCUSSION

To ensure the observed intracellular transport events were microtubule-based, an upright microscope was modified to operate in fluorescence and DIC modes simultaneously for visualizing both the plasmonic nanoprobe and the microtubules labeled with Oregon Green 488-tagged taxol molecules. The optical path of epi-fluorescence mode was superimposed onto that of DIC mode (Figure 1). The corresponding DIC and fluorescence images of the sample were collected simultaneously using the same microscope objective, then spectrally separated by a dichroic mirror and optical filters, and projected to different portions of the same camera's sensor array. Since there are no mechanical parts that need to be toggled in the optical path, the temporal resolution of the dual-modality microscope is determined solely by the signal intensity. In this setup, fluorescence images are slightly stretched by ~100 nm along the shear direction due to the second Nomarski prism in the optical path. This level of distortion is smaller than the diffraction limit of light and barely noticeable in a conventional epi-fluorescence microscope.

It is worth noting that, when taking DIC and fluorescence images of the same sample in an alternate manner, as is being done routinely in many cell and molecular biology laboratories, researchers need to switch the optical path between transmission mode and epi-fluorescence mode and replace optical filters when toggling between the two modes. The toggling procedure results in insufficient time resolution for many dynamic biological processes. Video-rate imaging in fluorescence and DIC modes simultaneously is nearly impossible when the microscope is operated in the mechanical toggling manner.

Dual-modality SPORT makes it possible to track the trajectories of fluorescently tagged biomolecules and the rotational motions of the rod-shaped plasmonic nanoprobe. This technique answers the increasing need for a live-cell imaging tool to monitor both biomolecules, through fluorescence microscopy, and nanoparticles and cell morphology, through DIC microscopy.

The gold nanorods with an average size of 25 nm × 73 nm were surface-modified with cell penetrating peptide from the HIV-1 protein Tat (residues 47-57: YGRKKRRQRRR).<sup>27–29</sup> These gold nanorods were internalized naturally by A549 human lung cancer cells to form the endocytic vesicles that were transported subsequently on the cytoskeleton tracks. To use a gold nanorod wrapped inside an endocytic vesicle as orientation reporter for intracellular transport, the nanorod should be stationary with respect to the vesicle on the time scale of the transport events. This requirement is indeed valid as we have demonstrated that the nanorods wrapped inside the endocytic vesicles generated nearly constant bright and dark DIC intensities while being transported linearly on the microtubules composed of 13 protofilaments.<sup>17</sup> If the nanorods were allowed to perform rotational Brownian motion inside the vesicles, their orientation would not be fixed.

The DIC illumination light was on all the time, but the fluorescence excitation was applied sparsely to minimize photobleaching. The camera was kept recording for both channels to capture any applicable images. Movie 1 shows a complete intracellular transport process of a nanorod-containing vesicle from the diffusion and docking until its detachment from the microtubule tracks. Figure 2a shows the overlapped DIC image of the cell and the fluorescence image of the microtubule network. The nanorod's trajectory (translational movement) was plotted in blue to show that the nanorod was transported on the microtubule tracks.

It should be noted that the main purpose of dual-modality SPORT is to dynamically colocalize fluorescently labeled biomolecules or cellular structures with gold nanorod probes within 3D cell body. Although the microtubules are relatively stationary and do not require dynamic imaging, simultaneous imaging in two modes provides another benefit of identifying the right microtubule track in the same vertical plane as the nanorod probe.

On the basis of the translational and rotational motions of the nanorod-containing vesicle, five different stages in this transport process are identified and labeled in Figure 3. We are able to draw more detailed physical pictures of each stage based on the rotational motions of the optically anisotropic gold nanorod probe.

In Stage 1, the bright and dark DIC intensities of the nanorod fluctuated drastically and the displacement trace in Figure 2b shows evident randomness, most likely representing rotational Brownian motion in limited space. The fast rotation slowed

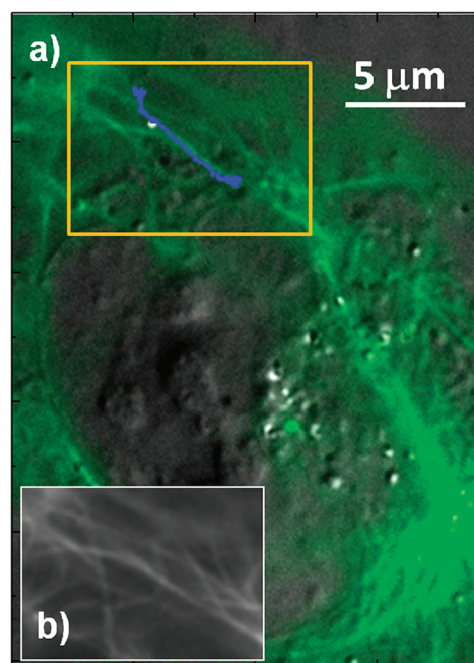


**Figure 2.** Cargo transport process in a living cell (movie, Supporting Information). (a) The overlapped DIC (gray) and fluorescence (green) images of the cell containing the gold nanorod probe. The green fluorescence shows the distribution of the microtubule network. The blue curve shows the intracellular transport trace of the nanorod-containing vesicle. (b) Fluorescence-only image of the region enclosed by the yellow frame.

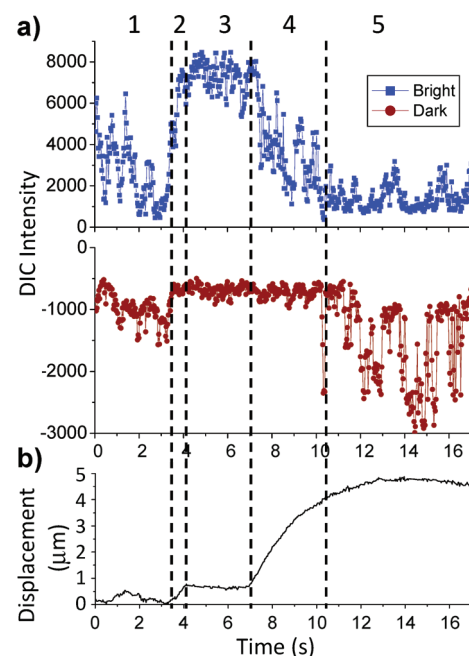


**Figure 3.** (a) DIC intensities as a function of time and (b) the absolute displacement of the gold nanorod-containing vesicle during the whole process, which is divided into 5 stages as labeled in the figure.

down gradually in the later part of Stage 1, indicating that a partial attachment of the nanorod-containing vesicle to the microtubule was established. At the end of Stage 1, the nanorod's DIC image showed a sudden change from almost completely dark to almost completely bright, followed by the active transport on the microtubule track in Stage 2. This change of



DIC image is an indication that the nanorod-containing vesicle experienced a  $\sim 90^\circ$  turn in the focal plane.<sup>17</sup> This reorientation before the transport may be ascribed to the pulling force generated by the motor proteins, and the vesicle changed from a partially relaxed state to a state under tension. In Stage 2, the nanorod was transported for 0.8  $\mu\text{m}$  with an average speed of  $\sim 1.0 \mu\text{m/s}$ , consistent with the reported values.<sup>30</sup> The constant bright image indicates that the nanorod's orientation did not change significantly during the transport, which is consistent with our previous observations.<sup>17</sup>

The vesicle paused for 3.0 s at the same location in Stage 3 and then resumed the transport in Stage 4. Contrary to the free rotation in Stage 1, the nanorod showed a nearly constant bright image, thus a fixed orientation, during the pause (Stage 3). The lack of free rotational motion cannot be explained by the steric hindrance alone. The cargo must be under tension to hold its orientation. Our observation depicts a new image that the cargo is tightly bound to the microtubule by multiple motor proteins with both directionalities (both kinesin and dynein) at the pauses. *It should be noted that it is only with SPORT that we are able to report whether the nanorod is rotating or not during the pausing state.*

In Stage 4, the vesicle was transported again on the microtubule tracks at the speed of  $\sim 1 \mu\text{m/s}$ . In Stage 5, the vesicle came closer to the nucleus, where it was more congested by the cellular organelles such as the microtubule-organizing center.<sup>31</sup> The transport became much slower. The nanorod finally stopped and restored the free rotation within a restricted location, indicating it was at a relaxed state with little tension applied on it.

The combined fluorescence and DIC images allow us to correlate the cargo's rotational behavior with the presence of the microtubule tracks. In Stage 1, the nanorod-containing vesicle started from an area where there was no visible microtubules and stopped on a piece of microtubule. The vesicle had a  $\sim 90^\circ$  turn, followed by the active transport on the microtubule, most likely representing the vesicle docking onto the microtubule and the pulling by the motor proteins. The directional transport in Stages 2 and 4 and the pause at Stage 3 happened all on the same microtubule. The nanorod kept the same orientation during the pause, indicating the nanorod was not detached from the microtubule. Further studies using dual-modality SPORT will lead to new live-cell observations for solving the intracellular transport mysteries, such as the question whether molecular motors with different directionalities work in coordination or fight a "tug of war" to reverse the transport direction.<sup>16,32,33</sup>

## CONCLUSION

In summary, the dual-modality SPORT technique was introduced for the simultaneous imaging of fluorescently tagged biomolecules and plasmonic nanorod probes in living cells at video rate. The potential of this technique has been demonstrated by visualizing the rotational dynamics of gold nanorod-containing vesicles at the transition stages, e.g., the cargo docking and undocking events and pauses, of the microtubule-based intracellular transport for the first time.

## ASSOCIATED CONTENT

### Supporting Information

A movie recorded at 32 frames per second to show a complete transport process of a nanorod-containing vesicle on the microtubule tracks. This material is available free of charge via the Internet at <http://pubs.acs.org>.

## AUTHOR INFORMATION

### Corresponding Author

\*E-mail: [nfang@iastate.edu](mailto:nfang@iastate.edu). Fax: (+1) 515-294-0105.

### Present Addresses

<sup>†</sup>Department of Chemistry, University of Washington, Seattle, WA 98195.

<sup>‡</sup>Department of Chemistry, North Carolina State University, Raleigh, NC 27695.

## ACKNOWLEDGMENTS

This work was supported by U.S. Department of Energy, Office of Basic Energy Sciences, Division of Chemical Sciences, Geosciences, and Biosciences through the Ames Laboratory. The Ames Laboratory is operated for the U.S. Department of Energy by Iowa State University under contract no. DE-AC02-07CH11358. Y.G. was also supported in part by Plant Science Institute at Iowa State University.

## REFERENCES

- (1) Lubyphe, K. *Curr. Opin. Cell Biol.* **1994**, *6*, 3.
- (2) Hirokawa, N. *Science* **1998**, *279*, 519.
- (3) Vale, R. D. *Cell* **2003**, *112*, 467.
- (4) Hirokawa, N.; Takemura, R. *Nat. Rev. Neurosci.* **2005**, *6*, 201.
- (5) Svoboda, K.; Schmidt, C. F.; Schnapp, B. J.; Block, S. M. *Nature* **1993**, *365*, 721.
- (6) Coy, D. L.; Wagenbach, M.; Howard, J. J. *Biol. Chem.* **1999**, *274*, 3667.
- (7) Reck-Peterson, S. L.; Yildiz, A.; Carter, A. P.; Gennerich, A.; Zhang, N.; Vale, R. D. *Cell* **2006**, *126*, 335.
- (8) Schnitzer, M. J.; Block, S. M. *Nature* **1997**, *388*, 386.
- (9) Khalil, A. S.; Appleyard, D. C.; Labno, A. K.; Georges, A.; Karplus, M.; Belcher, A. M.; Hwang, W.; Lang, M. J. *Proc. Natl. Acad. Sci. U. S. A.* **2008**, *105*, 19247.
- (10) Hancock, W. O.; Howard, J. J. *Cell Biol.* **1998**, *140*, 1395.
- (11) Ross, J. L.; Ali, M. Y.; Warshaw, D. M. *Curr. Opin. Cell Biol.* **2008**, *20*, 41.
- (12) Gennerich, A.; Vale, R. D. *Curr. Opin. Cell Biol.* **2009**, *21*, 59.
- (13) Block, S. M. *Biophys. J.* **2007**, *92*, 2986.
- (14) Sindelar, C. V.; Downing, K. H. *Proc. Natl. Acad. Sci. U. S. A.* **2010**, *107*, 4111.
- (15) Miller, K. E.; Heidemann, S. R. *Exp. Cell Res.* **2008**, *314*, 1981.
- (16) Kural, C.; Kim, H.; Syed, S.; Goshima, G.; Gelfand, V. I.; Selvin, P. R. *Science* **2005**, *308*, 1469.
- (17) Wang, G. F.; Sun, W.; Luo, Y.; Fang, N. *J. Am. Chem. Soc.* **2010**, *132*, 16417.
- (18) Ha, J. W.; Sun, W.; Wang, G.; Fang, N. *Chem. Commun.* **2011**, *47*, 7743.
- (19) Jana, N. R.; Gearheart, L.; Murphy, C. J. *J. Phys. Chem. B* **2001**, *105*, 4065.
- (20) Lee, K.-S.; El-Sayed, M. A. *J. Phys. Chem. B* **2006**, *110*, 19220.
- (21) Sonnichsen, C.; Alivisatos, A. P. *Nano Lett.* **2005**, *5*, 301.
- (22) Spetzler, D.; York, J.; Daniel, D.; Fromme, R.; Lowry, D.; Frasch, W. *Biochemistry* **2006**, *45*, 3117.
- (23) Pluta, M. *Advance light microscopy*; Elsevier Science Publishing Co. Inc.: New York, 1989; Vol. 2.
- (24) Sun, W.; Wang, G. F.; Fang, N.; Yeung, E. S. *Anal. Chem.* **2009**, *81*, 9203.
- (25) Tilney, L. G.; Bryan, J.; Bush, D. J.; Fujiwara, K.; Mooseker, M. S.; Murphy, D. B.; Snyder, D. H. *J. Cell Biol.* **1973**, *59*, 267.
- (26) Narayanan, R.; Lipert, R. J.; Porter, M. D. *Anal. Chem.* **2008**, *80*, 2265.
- (27) de la Fuente, J. M.; Berry, C. C. *Bioconjugate Chem.* **2005**, *16*, 1176.
- (28) Tkachenko, A. G.; Xie, H.; Liu, Y. L.; Coleman, D.; Ryan, J.; Glomm, W. R.; Shipton, M. K.; Franzen, S.; Feldheim, D. L. *Bioconjugate Chem.* **2004**, *15*, 482.

- (29) Heitz, F.; Morris, M. C.; Divita, G. *Br. J. Pharmacol.* **2009**, *157*, 195.
- (30) Cai, D. W.; Verhey, K. J.; Meyhofer, E. *Biophys. J.* **2007**, *92*, 4137.
- (31) Bailey, C. J.; Crystal, R. G.; Leopold, P. L. *J. Virol.* **2003**, *77*, 13275.
- (32) Gross, S. P.; Welte, M. A.; Block, S. M.; Wieschaus, E. F. *J. Cell Biol.* **2002**, *156*, 715.
- (33) Muller, M. J. I.; Klumpp, S.; Lipowsky, R. *Proc. Natl. Acad. Sci. U. S. A.* **2008**, *105*, 4609.